Desalination and Water Treatment
www.deswater.com

doi: 10.5004/dwt.2019.24115

154 (2019) 385–394
June

Application of *Momordica charantia* (bitter gourd) waste for the removal of malachite green dye from aqueous solution

Linda B.L. Lim[a,*], Namal Priyantha[b,c], Ke Jia Mek[a], Nur Afiqah Hazirah Mohamad Zaidi[a]

[a]*Department of Chemistry, Faculty of Science, Universiti Brunei Darussalam, Jalan Tungku Link, Gadong, Negara Brunei Darussalam, Tel. +00-673-8748010; emails: linda.lim@ubd.edu.bn (L.B.L. Lim), mek_ke_jia@hotmail.com (K.J. Mek), afhazirah@gmail.com (N.A.H. Mohamad Zaidi)*
[b]*Department of Chemistry, Faculty of Science, University of Peradeniya, Peradeniya, Sri Lanka, email: namal.priyantha@yahoo.com*
[c]*Postgraduate Institute of Science, University of Peradeniya, Peradeniya, Sri Lanka*

Received 24 September 2018; Accepted 9 March 2019

ABSTRACT

Momordica charantia (bitter gourd) waste (BGW) as a low-cost adsorbent was successfully used to remove malachite green (MG) dye from aqueous solution in batch adsorption experiment. BGW was characterized by scanning electron microscopy and Fourier transform infrared spectroscopy. Optimal experimental conditions were ascertained for contact time, medium pH and ionic strength. Of the six models used, adsorption isotherm studies confirmed that the Sips model fitted well to the experimental data. Maximum adsorption capacity (q_{max}) of BGW for MG dye based on the Langmuir and Sips models was 96.4 and 240.0 mg g^{-1}, respectively. The BGW–MG kinetics fitted well to the pseudo-second-order model. Adsorption of MG onto BGW was influenced, to some extent, by the presence of salts (KCl, KNO_3 and NaCl). Studies showed that 0.1 mol dm^{-3} NaOH was able to regenerate BGW and improve its adsorption capability to 95% dye removal at 1st cycle, and subsequently maintaining its high adsorption ability throughout the five consecutive cycles.

Keywords: Momordica charantia (Bitter gourd) adsorbent; Adsorption isotherm; Cationic dye; Malachite green dye; Regeneration

1. Introduction

In the olden days, prior to the existence of manufacturing industries, plants and animals were the sources of dyes used for dying textiles. However, with man-made synthetic dyes becoming more readily accessible, the use of these synthetic dyes has outweighed the natural dyes. As a result of growing population and booming industries, thousands of tons of dye wastewater are being discharged to the environment annually [1]. Therefore, from the environmental stand point, it is challenging to treat dye effluents because of their synthetic origins and complex aromatic structures, which are biologically non-degradable and many of these dyes are detrimental and toxic to health.

For wastewater treatment, adsorption technique has become more popular among the industries as it has been found to be superior to other techniques in terms of cost, simple design, ease of operation and insensitivity to toxic harmful substances [2]. As a result, numerous studies on agricultural wastes [3–8], fruit wastes [9–13] and industrial residues [14,15], and many others [16–21] have been tested for the removal of dyes and heavy metals from aqueous solutions. Despite many reported adsorbents, there is still a continuous search for better, cheaper and more effective low-cost adsorbents.

Malachite green (MG), whose structure is shown in Fig. 1, is a cationic dye that belongs to the class of triphenylmethane

* Corresponding author.

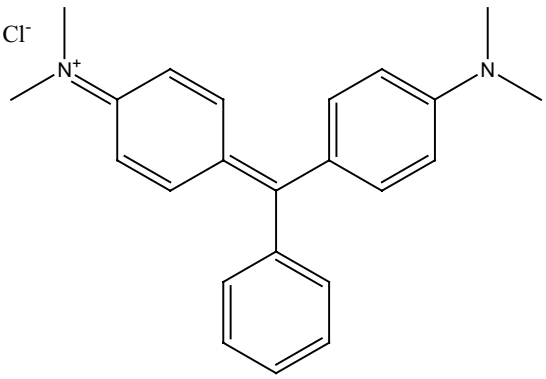

Fig. 1. Structure of malachite green dye.

dyes. MG appears as blue-green color in aqueous solution with a maximum absorbance at 618 nm. As it is widely used by textile industries to dye cotton, paper, silk and wool, the extensive usage of MG dye has been reported to cause damage to the liver, spleen, kidney and heart [22,23]. Hence, there is a need for it to be removed from wastewater as it poses a threat to human health.

Momordica charantia, otherwise known as bitter gourd, is very popular in Asia and South East Asia. In Brunei Darussalam, the flesh is usually fried or cooked as a curry dish while the center pith and seeds are being discarded as waste. Very few studies based on bitter gourd as an adsorbent in the treatment of wastewater were found. Main reports were on the use of bitter gourd peroxidase for the treatment of water contaminated with aromatic amines [24], phenols [25] and also for the removal of anthracene [26], while the removal of heavy metals from aqueous solutions was carried out using the bitter gourd seed powder [27]. To date, there is only one report on the use of bitter gourd waste (BGW) for the removal of crystal violet dye [28].

In this study, the focus was on the use of BGW as the adsorbent for the removal of MG dye from simulated aqueous solution containing the dye. The adsorption characteristics of BGW toward MG dye removal such as effects of pH, ionic strength, shaking time, were investigated. Data obtained from the batch adsorption studies were analyzed with various adsorption isotherm and kinetic models. Spent BGW was tested to see if BGW could be regenerated and reused. Such information would, therefore, provide insight as to whether BGW has the potential to be utilized as a low-cost adsorbent in the real life treatment of wastewater.

2. Materials and methods

2.1. Sample preparation and chemical reagents

The BGW, consisting of the inedible seeds and pith, was cleaned with distilled water and dried at 80°C in an oven until a constant mass was reached. The dried BGW sample was then blended and sieved to <355 μm particle size using laboratory metal sieves. Malachite green (MG) (molecular formula $C_{23}H_{25}ClN_2$, molecular weight 364.91 g mol^{-1}) was purchased from Sigma-Aldrich (USA), and used without further purification.

2.2. Adsorption studies

Optimization of parameters for contact time (0–240 min), pH (3–8), effect of salt concentration (0–1 mol dm^{-3} salt) and batch adsorption experiments for isotherm (0–1,000 mg L^{-1} MG) and kinetics (100 and 500 mg L^{-1} MG) were carried out following the methods as described by Dahri et al. [29] with slight modification. Agitation of the mixture was performed using the Stuart Scientific Flask Shaker SF1 (UK) with speed of 250 rpm at room temperature. All experiments were carried out in duplicate with the mixture of adsorbent–MG solution in ratio 1:500 (weight:volume), unless otherwise stated, and the average data are presented. The absorbance of MG dye was recorded at wavelength of 618 nm using the Shimadzu UV-1601PC spectrophotometer (Japan). The determination of the concentration of MG in each solution before and after adsorption experiments was performed with the aid of a properly constructed calibration curve of at least five standard MG solutions whose linear dynamic range included the concentration of MG to be determined.

2.3. Regeneration studies

Regeneration of the adsorption capacity of BGW was studied according to the procedure as described by Chieng et al. [30] using three different washing solutions (distilled water, 0.1 mol dm^{-3} HNO_3 and 0.1 mol dm^{-3} NaOH). Briefly, the adsorbent (1.0 g) was treated with 100 mg L^{-1} MG and the mixture was shaken at its optimum shaking time. After the shaking process, the mixture was filtered, the spent adsorbent was collected and dried in an oven as preparation to study the ability of BGW in adsorbing MG for several cycles. The dried dye loaded sample was divided into four fractions and three of them were treated by using the stated washing solutions. The mixture of the spent sample and the washing solution was shaken for 1.5 h, filtered and washed further by using distilled water until the color of the filtrates disappeared. The washed adsorbents were thereafter placed back in an oven. A fraction of the spent adsorbents was kept untouched to be used as a control for the next adsorption process. Another cycle of adsorption for the four fractions of the spent adsorbent was then continued and the regeneration studies were carried for five consecutive cycles.

2.4. Characterization of adsorbent

The Tescan Vega XMU (Czech Republic) scanning electron microscope was used for surface morphological analysis of BGW and dye-treated adsorbent (samples were prior coated with gold). Three different samples (original adsorbent, the dye-treated adsorbent and dye solid) were analyzed by Fourier transform infrared (FTIR) spectroscopy to determine the presence of functional groups.

3. Results and discussion

3.1. Optimization of parameters for contact time, medium pH and effect of salt concentration

The adsorption of MG was studied as a function of contact time in order to determine the time required for the

BGW–MG system to reach equilibrium. Rapid adsorption of MG occurred within the first half an hour (Fig. 2), which is most likely due to the fact that initially all the sites on the adsorbent's surface were vacant and the solute concentration gradient was high. Over time, these active sites are gradually being filled, thereby resulting in the slowing down of the adsorption process of MG until an equilibrium is eventually reached. According to Fig. 2, it is clear that 3 h of shaking were sufficient to ensure complete equilibrium of the BGW–MG system.

The pH factor is very crucial in dye adsorption studies, where it affects both the degree of ionization of the dye and the surface properties of the adsorbent [31]. As a result, the ability of an adsorbent to adsorb dye would vary with the pH of the medium. BGW showed a 37.8% dye removal at the untreated pH (3.6) of 100 mg L^{-1} MG dye (Fig. 3). The adsorption capacity of BGW increased with increase in solution pH and the maximum adsorption for MG was observed at pH 8, as depicted in Fig. 3. At high OH^- ions concentration, deprotonation of the surface functional groups can take place causing the adsorbent's surface to be more negatively charged when the solution pH increases. Therefore, electrostatic interaction between negatively charged adsorbent's surface and cationic MG molecules could account for the observed increase in adsorption. Furthermore, when the solution pH is above the zero point of charge (pH_{pzc} = 5.5) [28], the negative charge density on the surface of BGW increases favoring the adsorption of the cationic dye.

Dahri et al [8] reported that at extreme pH (2 and 10), the adsorption intensity of MG was greatly affected. Hence, the study range was limited to pH between 3 and 8 and no pH adjustment was made as to avoid error resulted from the reduction of intensity by the change of pH.

Wastewater effluent commonly contains higher salt concentration which makes it necessary to study the effects of ionic strength on the adsorption of dye. The salts, NaCl, KCl and KNO_3, were chosen as the understudied salts and the adsorption of MG was investigated at different salt concentrations ranging from 0 to 1 mol dm^{-3}. It was observed (Fig. 4) that of the three salts, NaCl showed the greatest reduction whereby the adsorption capacity decreased to ~13% and eventually reached a constant value with increased concentration of NaCl in the medium. This can be due to the presence of Na^+ ions which competes with the MG cationic dye for the sites available for adsorption. Unlike NaCl, both KCl and KNO_3 initially showed a decrease in adsorbing efficiency, after which the removal of MG was increased as the concentration of salts increased in the dye solution. The observed increase in the adsorption of MG dye could be due to the presence of anions from the salts causing electrostatic repulsion [32]. Similar behavior was also reported for the removal of crystal violet dye with BGW [28].

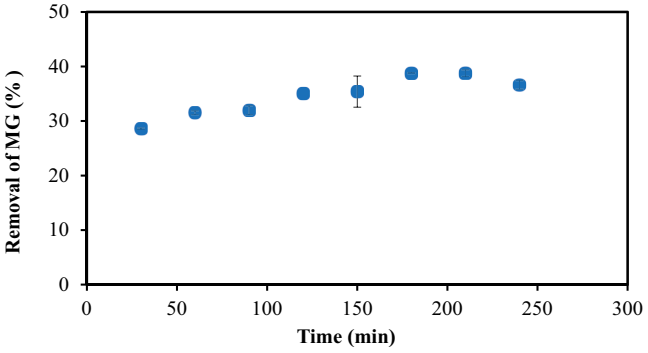

Fig. 2. Contact time required for the BGW–MG system to reach equilibrium (mass of BGW = 0.050 g; volume of MG solution = 25.0 mL; concentration of MG = 100 mg L^{-1}).

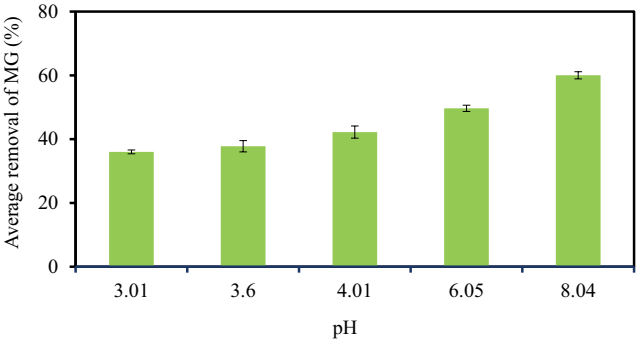

Fig. 3. Adsorption of MG onto BGW in different medium pH (mass of BGW = 0.050 g; volume of MG solution = 25 mL; concentration of MG = 100 mg L^{-1}).

3.2. Adsorption isotherm

Investigation of the adsorption ability of BGW toward MG dye was carried out by batch adsorption isotherm studies. The results were further evaluated by fitting the experimental data obtained to five different adsorption isotherm models namely Langmuir [33], Freundlich [34], Temkin [35], Sips [36] and Redlich–Peterson (R-P) [37] models (Table 1) in order to determine the best fit isotherm model for the removal of dye by the BGW.

Briefly, the Langmuir isotherm model is valid for monolayer adsorption onto a homogenous surface while the Freundlich model is suitable for the adsorption on heterogeneous surface and multilayer adsorption to the binding sites on the surface of the adsorbent. The Temkin model depicts a linear decrease of heat of adsorption with increasing surface coverage due to the adsorbate–adsorbent interactions.

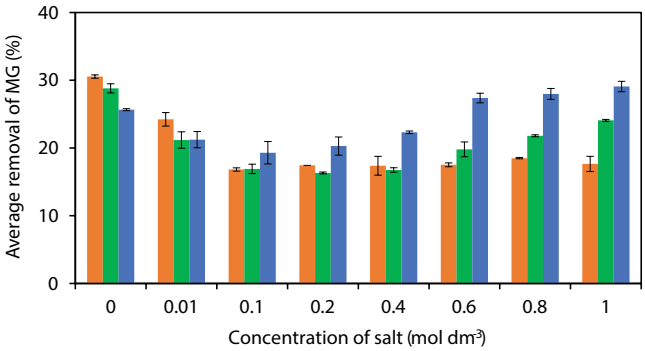

Fig. 4. Effect of ionic strength using NaCl (■), KCl (■) and KNO_3 (■) (0.050 g of BGW; 25.0 mL of 100 mg L^{-1} MG solution).

Table 1
Linearized isotherm models with their linearized equations and their corresponding plots

Adsorption isotherm model	Linearized isotherm equation	Linear plot
Langmuir	$\frac{C_e}{q_e}=\frac{1}{K_L q_{\max}}+\frac{C_e}{q_{\max}}$	$\frac{C_e}{q_e}$ *vs* C_e
Freundlich	$\log q_e=\frac{1}{n}\log C_e+\log K_F$	$\log q_e$ *vs* $\log C_e$
Temkin	$q_e=\left(\frac{RT}{b_T}\right)\ln K_T+\left(\frac{RT}{b_T}\right)\ln C_e$	q_e *vs* $\ln C_e$
Sips	$\ln\left(\frac{q_e}{q_{\max}-q_e}\right)=\frac{1}{n}\ln C_e+\ln K_S$	$\ln\left(\frac{q_e}{q_{\max}-q_e}\right)$ *vs* $\ln C_e$
Redlich–Peterson (R-P)	$\ln\left(\frac{K_R C_e}{q_e}-1\right)=n\ln C_e+\ln a_R$	$\ln\left(\frac{K_R C_e}{q_e}-1\right)$ *vs* $\ln C_e$

$q_{\max}$ is the maximum adsorption capacity; K_L (L mg^{-1}), K_F (mg g^{-1} (L mg^{-1})$^{1/n}$), K_T (L mg^{-1}), K_S (L mg^{-1}) and K_R (L g^{-1}) are the isotherm constants with respect to the Langmuir, Freundlich, Temkin, Sips and R-P isotherm models, respectively; n is the empirical parameter which is related to the adsorption intensity; q_e is the amount of dye adsorbed (mg g^{-1}); C_e is the equilibrium dye concentration in solution (mg L^{-1}); $1/n$ is the Sips model exponent; a_R (L mg^{-1}) is the R-P constant.

However, the R-P model incorporates three parameters into an empirical model combining the features of both the Freundlich and Langmuir isotherm models. Similarly, the Sips model is also a combination of both the Freundlich and Langmuir models. When the concentration of adsorbate approaches a low value, the Sips isotherm effectively reduces to Freundlich and reduces to the Langmuir monolayer adsorption characteristic at high adsorbate concentration.

Determination of the best fit isotherm model was based on three criteria namely (1) highest regression coefficient, R^2, (2) comparison of experiment isotherm data with simulation plots and (3) error analyses using six error functions whose equations are shown in Table 2.

Table 3 shows that of the five isotherm models employed to describe the adsorption process of MG dye onto BGW, the Sips model has the best fit based on its highest value of linear regression coefficient (R^2), followed by Freundlich > Langmuir > R-P > Temkin models. These observations are in line with the simulated plots, as shown in Fig. 5, where the Temkin model clearly deviated from the experimental isotherm data, thereby indicating its unsuitability to describe the adsorption of MG onto BGW. According to the results from the error analyses, as shown in Table 3, the Sips model is overall the best fit model which leads to the maximum adsorption capacity ($q_{\max}$) of 240.0 mg g^{-1} for MG adsorption onto BGW.

Table 4 shows a comparison of $q_{\max}$ values of different adsorbents reported for the removal of MG dye. It can be observed that BGW shows a much better adsorption capacity than many other low-cost adsorbents do, and its value is comparable with some of the modified adsorbents reported. Another important aspect is that BGW used in this study was not subjected to any activation or surface modification, except only oven drying at 80°C. Therefore, BGW still has the potential to further enhance its adsorption capacity through physical activation and chemical surface modification.

The removal of MG dye was performed at five different temperatures at 298, 313, 323, 333 and 343 K using three different dye concentrations (100, 300, and 500 mg L^{-1}) for the determination of thermodynamic parameters as shown in Fig. 6. The parameters were obtained with the following equations with the aid of Fig. 7 [52].

$$\Delta G^\circ=\Delta H^\circ-T\Delta S^\circ \tag{1}$$

Table 2
A total of six error functions used

Type of errors	Equations
Average relative error (ARE)	$\frac{100}{n}\sum_{i=1}^{n}\left\lvert\frac{q_{e,\text{meas}}-q_{e,\text{cal}}}{q_{e,\text{meas}}}\right\rvert_i$
Hybrid fractional error function (HYBRID)	$\frac{100}{n-p}\sum_{i=1}^{n}\left[\frac{\left(q_{e,\text{meas}}-q_{e,\text{cal}}\right)^2}{q_{e,\text{meas}}}\right]_i$
Sum of absolute error (EABS)	$\sum_{i=1}^{n}\left\lvert q_{e,\text{meas}}-q_{e,\text{cal}}\right\rvert$
Marquardt's percent standard deviation (MPSD)	$100\sqrt{\frac{1}{n-p}\sum_{i=1}^{n}\left(\frac{q_{e,\text{meas}}-q_{e,\text{cal}}}{q_{e,\text{meas}}}\right)_i^2}$
Non-linear chi-square test (χ^2)	$\sum_{i=1}^{n}\frac{\left(q_{e,\text{meas}}-q_{e,\text{cal}}\right)^2}{q_{e,\text{meas}}}$

$q_{e,\text{meas}}$ is the experimental value, $q_{e,\text{cal}}$ is the calculated value, n is the number of data points in the experiment and p is the number of parameters of the model.

Table 3
Adsorption isotherm parameters of MG dye for different models and their error values

Model	Value	ARE	HYBRID	EABS	MPSD	χ^2
Langmuir		19.96	76.75	40.96	24.96	18.76
q_{max} (mg g^{-1})	96.4					
K_L (L mg^{-1})	0.005					
R^2	0.9623					
Freundlich		10.74	41.77	33.00	13.85	28.35
K_F (mg$^{1-1/n}$ L$^{1/n}$ g^{-1})	1.61					
n	1.69					
R^2	0.9819					
Temkin		98.48	1,527.68	128.99	174.11	63.81
K_T (L mg^{-1})	0.11					
b_T (J mol^{-1})	158.56					
R^2	0.8963					
Sips		10.74	42.18	31.60	15.04	24.38
q_{max} (mg g^{-1})	240.00					
K_S (L mg^{-1})	0.01					
$1/n$	0.67					
n	1.49					
R^2	0.9828					
Redlich–Peterson		10.75	45.35	32.99	14.33	28.28
K_R (L g^{-1})	50.00					
α	0.41					
a_R (L mg^{-1})	30.44					
R^2	0.9621					

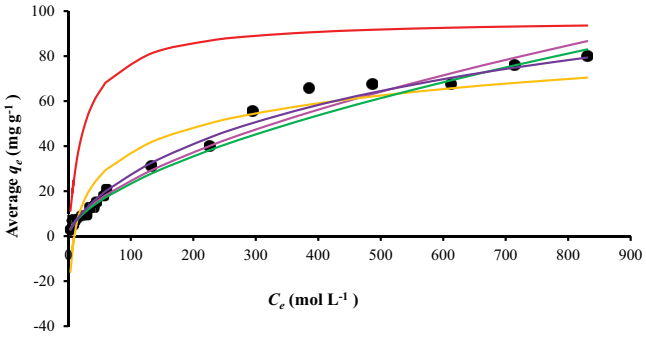

Fig. 5. Comparison of simulation plots between the various isotherm models of Langmuir (—), Freundlich (—), Temkin (—), R-P (—) and Sips (—) with experimental data (●) (mass of BGW = 0.050 g; volume of MG solution = 25.0 mL; concentration of MG = 0–1,000 mg L^{-1}).

$$\Delta G^{\circ} = -RT\ln K \quad (2)$$

$$K = \frac{C_s}{C_e} \quad (3)$$

$$\ln K = \frac{\Delta S^{\circ}}{R} - \frac{\Delta H^{\circ}}{RT} \quad (4)$$

Table 4
BGW and a list of selected reported adsorbents with their q_{max} values for the adsorption of MG dye

Adsorbent	q_{max} (mg g^{-1})	Reference
Bitter gourd waste	240.0 (Sips)	This work
	96.4 (Langmuir)	This work
Walnut shell	90.8	[7]
SDS-treated *Artocarpus odoratissimus* skin	100.8	[11]
EDTA-treated *Artocarpus odoratissimus* skin	116.8	[11]
NaOH-treated *Artocarpus odoratissimus* skin	157.6	[11]
Artocarpus odoratissimus leaves	254.9	[18]
Casuarina equisetifolia needle	77.6	[29]
Leaves of *Solanum tuberosum*	33.3	[38]
Wood apple shell	34.6	[39]
Mango seed husks	47.9	[40]
Lemon peel	51.7	[41]
Rattan sawdust	62.7	[42]
Azolla pinnata	87.0	[43]
H_3PO_4-treated *Azolla pinnata*	292.1	[43]
NaOH-treated *Azolla pinnata*	109.6	[43]
Rice straw char	148.7	[44]
Modified rice straw	282.5	[45]
Peat	143.7	[46]
Nanoparticles synthesized on the ash produced from the leaves of *Rosa canina* L.	500.0	[47]
Activated carbon	509.0	[48]
Chemically modified breadnut peel	353.0	[49]
Artocarpus altilis (Breadfruit) skin	55.2	[50]
Jackfruit seeds	66.0	[51]

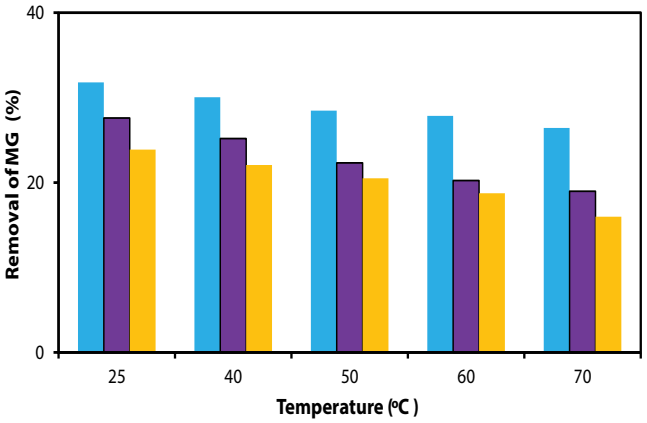

Fig. 6. Adsorption of MG onto BGW at 100 mg L^{-1} (■), 300 mg L^{-1} (■) and 500 mg L^{-1} (■) MG concentrations (0.050 g of BGW in 25.0 mL of MG) at different temperatures.

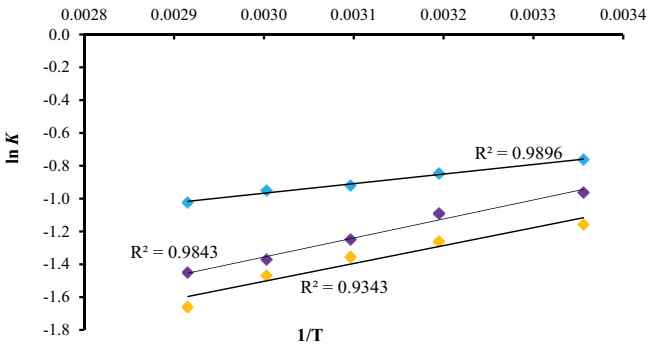

Fig. 7. Van't Hoff plots for the adsorption of MG onto BGW at 100 mg L^{-1} (♦), 300 mg L^{-1} (♦) and 500 mg L^{-1} (♦) MG concentrations (0.050 g of BGW in 25.0 mL of MG).

where $\Delta G°$ is the Gibbs free energy, $\Delta H°$ is the enthalpy change, $\Delta S°$ is the entropy change, T is the temperature in Kelvin (K), K being the adsorption distribution coefficient, C_s is the adsorbed dye concentration at equilibrium (mg L^{-1}), C_e is the remaining dye concentration in solution at equilibrium (mg L^{-1}), and R is the gas constant (J mol^{-1} K^{-1}). The thermodynamic parameters evaluated are given in Table 5.

Increasing positive values of $\Delta G°$ were obtained with temperature in the adsorption of MG indicating that the adsorption process is favored at lower temperatures. The entropy ($\Delta S°$) values were also found to be negative for all the three concentrations of MG dyes investigated with increasing temperature from 298 to 343 K, thereby suggesting that there may be an increased orderliness in the system. Further, the adsorption of MG is exothermic process, as indicated by the negative $\Delta H°$ values.

3.3. Adsorption kinetics of MG onto BGW

In order to investigate the potential rate-controlling steps involved in the process of adsorption, the experimental data were fitted onto two kinetic models namely the Lagergren pseudo-first-order [53] and pseudo-second-order [54] with their linear equations as shown below.

Pseudo-first-order:

$$\log\left(q_e - q_t\right) = \log\left(q_{e,\mathrm{cal}}\right) - \frac{k_1}{2.303}t \tag{5}$$

Pseudo-second-order:

$$\frac{t}{q_t} = \frac{q}{k_2 q_e^2} + \frac{1}{q_e}t \tag{6}$$

where q_e and q_t are the amount of dye adsorbed (mg g^{-1}) at equilibrium and at time t, respectively, and k_1 (min^{-1}) and k_2 (g mg^{-1} min^{-1}) are the rate constants of adsorption for pseudo-first and pseudo-second-order kinetics, respectively.

Under the experimental conditions employed, simulation plots of kinetics data from experiment for both dye concentrations are closer fitted to that of the pseudo-second-order kinetics, as can be seen from Fig. 8. This can be further confirmed by the higher R^2 (Fig. 9), lower error values and compatible $q_{e,\mathrm{cal}}$ and $q_{e,\mathrm{expt}}$ values (Table 6) as compared with the pseudo-first-order. Hence, it can be concluded that the adsorption of MG onto BGW follows the pseudo-second-order kinetics. The decrease in rate constant k_2 with increasing concentration of MG is also in line with literature where equilibrium will be reached at longer time when higher initial dye concentration is used [55].

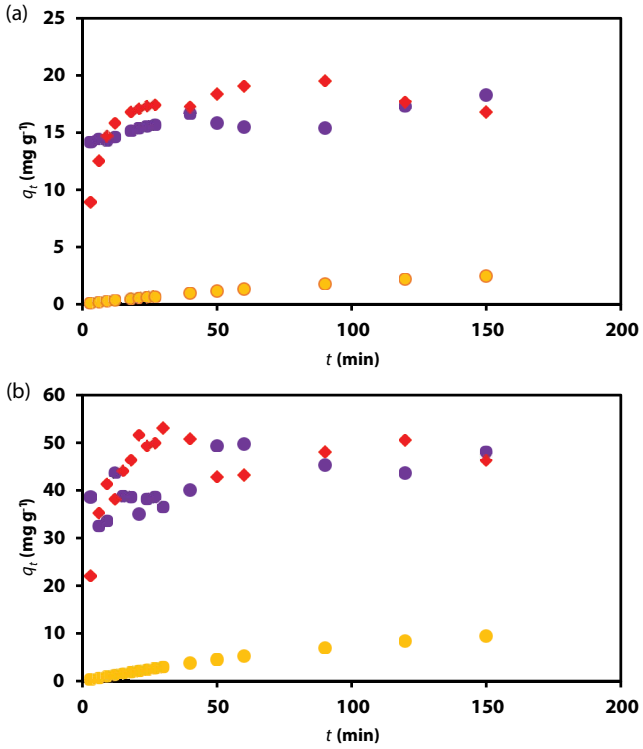

Fig. 8. Comparison of kinetics experiment data (●) with pseudo-first (●) and pseudo-second (♦) order kinetics for the adsorption of MG onto BGW at 100 mg L^{-1} (a) and 500 mg L^{-1} (b) (mass of BGW = 0.050 g; volume of MG solution = 25.0 mL).

Table 5
Thermodynamic parameter values for the adsorption of MG onto BGW

Conc. (mg L^{-1})	$\Delta H°$ (kJ mol^{-1})	$\Delta S°$ (J mol^{-1} K^{-1})	$\Delta G°$ (kJ mol^{-1})					R^2
			298 K	313 K	323 K	333 K	343 K	
100	–4.85	–22.59	1.89	2.20	2.47	2.64	2.92	0.990
300	–9.64	–40.19	2.39	2.83	3.35	3.80	4.14	0.984
500	–9.07	–39.70	2.87	3.28	3.64	4.06	4.73	0.934

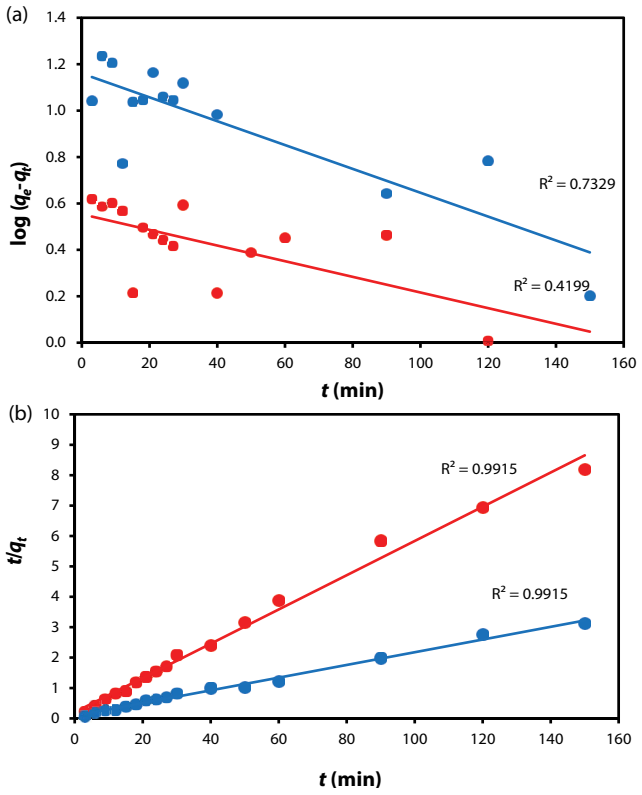

Fig. 9. Linear plots of Lagergren pseudo-first order (a) and pseudo-second-order (b) models for the adsorption of MG onto BGW at 100 mg L^{-1} (●) and 500 mg L^{-1} (●) MG concentrations (mass of BGW = 0.050 g; volume of MG solution = 25.0 mL).

Table 6
Kinetic parameters and error values for the adsorption of MG onto BGW at two different dye concentrations

Concentration (mg L^{-1})	100	500
Pseudo-first-order kinetics		
ARE	88.76	81.77
HYBRID	1,479.28	3,419.52
EABS	252.02	595.41
MPSD	76.03	72.30
χ^2	236.68	547.12
k_1 (min^{-1})	0.008	0.012
R^2	0.4199	0.7329
$q_{e,cal}$ (mg g^{-1})	3.58	14.45
Pseudo-second-order kinetics		
ARE	13.11	19.50
HYBRID	45.14	249.39
EABS	36.70	136.66
MPSD	16.24	24.20
χ^2	7.22	39.90
k_2 (g mg^{-1} min^{-1})	0.016	0.005
R^2	0.9915	0.9915
$q_{e,cal}$ (mg g^{-1})	17.75	47.80
$q_{e,exp}$ (mg g^{-1})	20.78	69.63

3.4. Regeneration of spent BGW

In this study, MG dye-loaded BGW were subjected to three different treatments, that is, with HCl, NaOH and washing with distilled water. A control for comparison was prepared. Fig. 10 shows that at the 5th cycle, maximum reduction was observed for the control experiment followed by the spent BGW which was subjected to washing with distilled water. A reduction of ~4% was observed at the 5th cycle in treatment with HCl, indicating that the spent BGW can be regenerated and reused. Among the three methods studied, NaOH treatment was found to be the best for regeneration maintaining >95% removal throughout the five cycles. Although base treatment, in general, leads to enhanced removal for cationic dyes partly due to deprotonation of functional groups present in the adsorbent [56], the observation made that NaOH treatment of BGW shows the best regeneration ability which can be explained due to the fact that the adsorbent could be denatured during the treatment with 0.1 M NaOH solutions, thereby significantly changing adsorption characteristics.

3.5. Characterization of BGW

The scanning electron microscopy (SEM) micrographs of BGW at ~500× magnification showed that the surface of BGW (Fig. 11a) is a combination of both smooth and rough texture and many irregular folds were present within the rough surface, which could increase the surface area and be potential active adsorption sites for the adsorption of dye. After treatment with MG, the surface of BGW clearly shows a distinct difference (Fig. 11b), indicating that the dye molecules have adsorbed onto the surface of BGW.

The FTIR spectra of MG-treated BGW when compared with that of untreated BGW are shown in Fig. 12, while Fig. 13 is the comparison between the MG dye and the BGW loaded with MG dye. The broad peak at 3,391 cm^{-1} represents OH and NH stretching vibration whereas the peak at 1,650 cm^{-1} represent the C=C group. The carbonyl group (C=O) is seen at 1,743 cm^{-1}. After treatment with MG dye, the broad peaks of C=C and C=O were shifted to 3,356, 1,658 and 1,744 cm^{-1}, respectively.

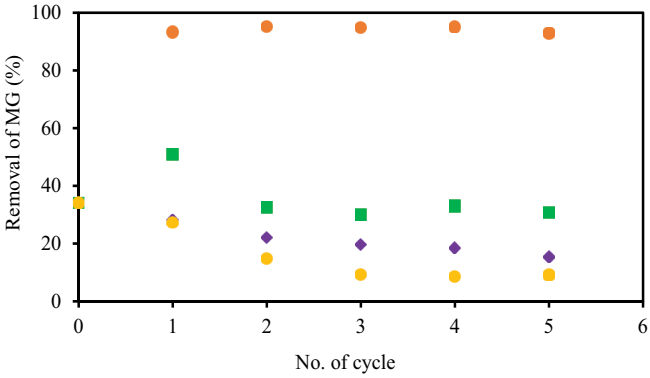

Fig. 10. Regeneration of BGW showing five consecutive cycles using different treatment methods: HCl (■), NaOH (●), H_2O (◆) and control (●) (mass of BGW = 0.050 g; concentration of MG = 100 mg L^{-1}).

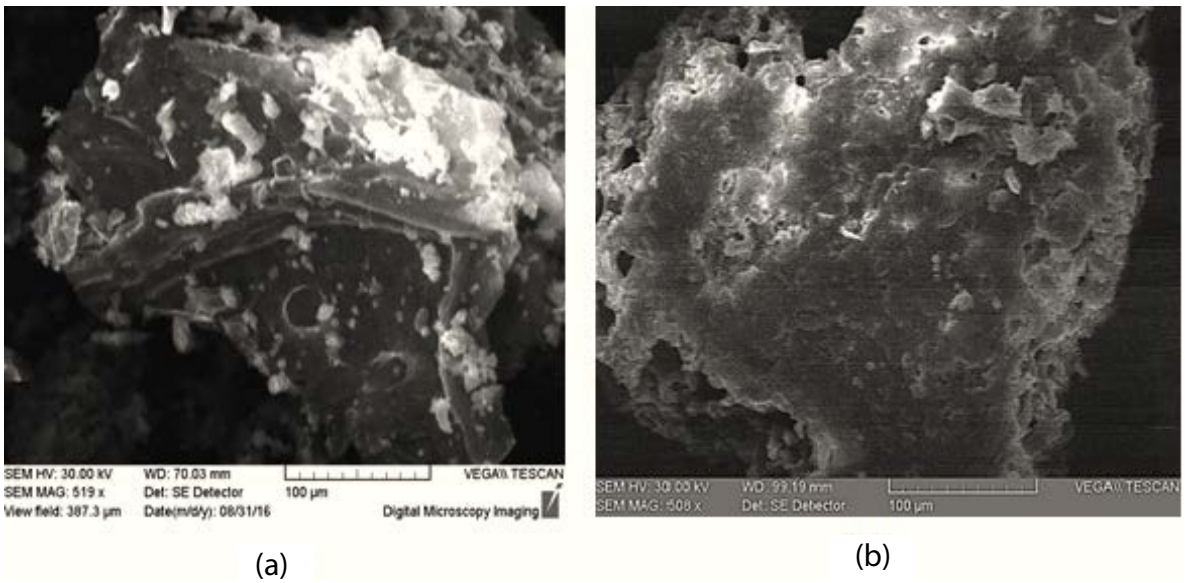

Fig. 11. Surface morphology of BGW (a) before and (b) after treatment with MG dye at 500× magnification.

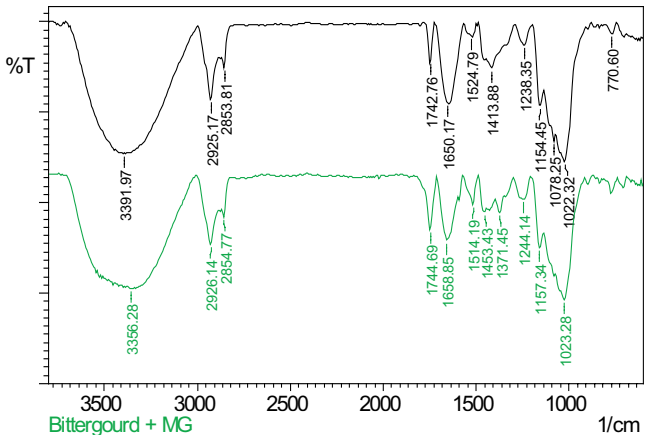

Fig. 12. FTIR spectra for functional group characterization of BGW (top black) and BGW–MG (bottom green).

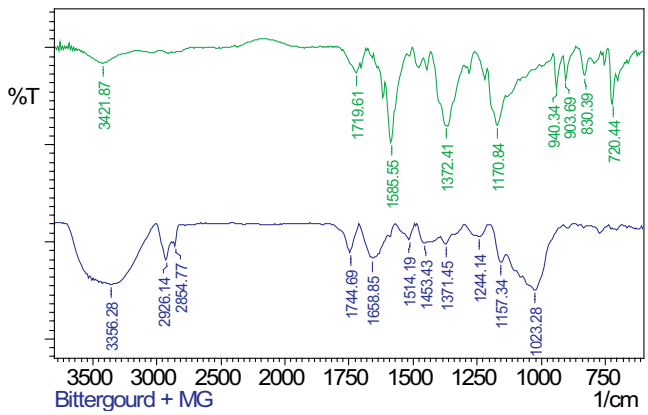

Fig. 13. FTIR spectra for functional group characterization of MG (top green) and BGW–MG (bottom blue).

The positive indication of the adsorption of MG onto BGW is the appearance of bands of C=C stretch of benzene ring and C–N stretch of aromatic tertiary amine at 1,586 and 1,371 cm^{-1}, respectively. The resulting prominent shifts indicate that these functional groups might be involved in the adsorption of MG onto the BGW's surface.

4. Conclusion

This study concludes that the BGW has the potential to act as an adsorbent for malachite green (MG) dye based on its high maximum adsorption capacity of 240.0 mg g^{-1} as determined by the Sips isotherm model, the most suitable model according to regression coefficient and error functions. The adsorption capacity can be further enhanced when the adsorbent is treated under basic conditions. The presence of salts, especially NaCl, influenced the adsorption of MG onto BGW. The adsorption kinetic data were best described by the pseudo-second-order kinetics. Regeneration experiments showed that BGW has the potential to be regenerated and reused while maintaining its ability to adsorb especially under both acidic and basic conditions, adding to its value as a potential low-cost adsorbent.

Acknowledgments

The authors would like to thank the Government of Negara Brunei Darussalam, the Universiti Brunei Darussalam and CAMES for their continuous support.

References

[1] Z. Aksu, Application of biosorption for the removal of organic pollutants: a review, Process Biochem., 40 (2005) 997–1026.
[2] V.K. Garg, R. Kumar, R. Gupta, Removal of malachite green dye from aqueous solution by adsorption using agro-industry waste: a case study of *Prosopis cineraria*, Dyes Pigm., 62 (2004) 1–10.
[3] K.A. Adegoke, O.S. Bello, Dye sequestration using agricultural wastes as adsorbents, Water Resour. Ind., 12 (2015) 8–24.

[4] S. Rangabhashiyam, N. Anu, N. Selvaraju, Sequestration of dye from textile industry wastewater using agricultural waste products as adsorbents, J. Environ. Chem. Eng., 1 (2013) 629–641.
[5] H. Singh, G. Chauhan, A.K. Jain, S.K. Sharma, Adsorptive potential of agricultural wastes for removal of dyes from aqueous solutions, J. Environ. Chem. Eng., 5 (2017) 122–135.
[6] B.H. Hameed, A.A. Ahmad, Batch adsorption of methylene blue from aqueous solution by garlic peel, an agricultural waste biomass, J. Hazard. Mater., 164 (2009) 870–875.
[7] C. Namasivayam, D. Kavitha, Removal of Congo Red from water by adsorption onto activated carbon prepared from coir pith, an agricultural solid waste, Dyes Pigm., 54 (2002) 47–58.
[8] M.K. Dahri, M.R.R. Kooh, L.B.L. Lim, Water remediation using low cost adsorbent walnut shell for removal of malachite green: equilibrium, kinetics, thermodynamic and regeneration studies, J. Environ. Chem. Eng., 2 (2014) 1434–1444.
[9] W.S. Alencar, E. Acayanka, E.C. Lima, B. Royer, F.E. de Souza, J. Lameira, C.N. Alves, Application of *Mangifera indica* (mango) seeds as a biosorbent for removal of Victazol Orange 3R dye from aqueous solution and study of the biosorption mechanism, Chem. Eng. J., 209 (2012) 577–588.
[10] S. Chakraborty, S. Chowdhury, P.D. Saha, Insight into biosorption equilibrium, kinetics and thermodynamics of crystal violet onto *Ananas comosus* (pineapple) leaf powder, Appl. Water Sci., 2 (2012) 135–141.
[11] L.B.L. Lim, N. Priyantha, N.A.H.M. Zaidi, U.A.N. Jamil, H.I. Chieng, T. Zehra, A. Liyandeniya, Chemical modification of *Artocarpus odoratissimus* skin for enhancement of their adsorption capacities toward toxic malachite green dye, J. Mater. Environ. Sci., 7 (2016) 3211–3224.
[12] M.K. Dahri, L.B.L. Lim, C.C. Mei, Cempedak durian as a potential biosorbent for the removal of Brilliant Green dye from aqueous solution: equilibrium, thermodynamics and kinetics studies, Environ. Monit. Assess., 187 (2015) 546.
[13] D.L. Postai, C.A. Rodrigues, Adsorption of cationic dyes using waste from fruits of *Eugenia umbelliflora* Berg (Myrtaceae), Arabian J. Sci. Eng., 43 (2018) 2425–2440.
[14] G. Orlandi, J. Cavasotto, F.R.S. Machado Jr., G.L. Colpani, J.D. Magro, F. Dalcanton, J.M.M. Mello, M.A. Fiori, An adsorbent with a high adsorption capacity obtained from the cellulose sludge of industrial residues, Chemosphere, 169 (2017) 171–180.
[15] I. Anastopoulos, M. Karamesouti, A.C. Mitropoulos, G.Z. Kyzas, A review for coffee adsorbents, J. Mol. Liq., 229 (2017) 555–565.
[16] H.I. Chieng, L.B.L. Lim, N. Priyantha, Sorption characteristics of peat from Brunei Darussalam for the removal of rhodamine B dye from aqueous solution: adsorption isotherms, thermodynamics, kinetics and regeneration studies, Desal. Wat. Treat., 55 (2015) 664–677.
[17] N.A.H.M. Zaidi, L.B.L. Lim, N. Priyantha, A. Usman, *Artocarpus odoratissimus* leaves as an eco-friendly adsorbent for the removal of toxic rhodamine b dye in aqueous solution: equilibrium isotherm, kinetics, thermodynamics and regeneration studies, Arabian J. Sci. Eng., 43 (2018) 6011–6020.
[18] N.A.H.M. Zaidi, L.B.L. Lim, A. Usman, M.R.R. Kooh, Efficient adsorption of malachite green dye using *Artocarpus odoratissimus* leaves with artificial neural network modelling, Desal. Wat. Treat., 101 (2018) 313–324.
[19] R. Ahmad, I. Hasan, A. Mittal, Adsorption of Cr (VI) and Cd (II) on chitosan grafted polyaniline-OMMT nanocomposite: isotherms, kinetics and thermodynamics studies, Desal. Wat. Treat., 58 (2017) 144–153.
[20] H. Daraei, A. Mittal, Investigation of adsorption performance of activated carbon prepared from waste tire for the removal of methylene blue dye from wastewater, Desal. Wat. Treat., 90 (2017) 294–298.
[21] H.I. Chieng, L.B.L. Lim, N. Priyantha, D.T.B. Tennakoon, Sorption characteristics of peat of Brunei Darussalam III: equilibrium and kinetics studies on adsorption of crystal violet (CV), Int. J. Earth Sci. Eng., 6 (2013) 791–801.
[22] S. Srivastava, R. Sinha, D. Roy, Toxicological effects of malachite green, Aquat. Toxicol., 66 (2004) 319–329.
[23] A. Mittal, Adsorption kinetics of removal of a toxic dye, Malachite Green, from wastewater by using hen feathers, J. Hazard. Mater., 133 (2006) 196–202.
[24] Z. Karim, Q. Husain, Redox-mediated oxidation and removal of aromatic amines from polluted water by partially purified bitter gourd (*Momordica charantia*) peroxidase, Int. Biodeterior. Biodegrad., 63 (2009) 587–593.
[25] S. Akhtar, Q. Husain, Potential applications of immobilized bitter gourd (*Momordica charantia*) peroxidase in the removal of phenols from polluted water, Chemosphere, 65 (2006) 1228–1235.
[26] Z. Karim, Q. Husain, Removal of anthracene from model wastewater by immobilized peroxidase from *Momordica charantia* in batch process as well as in a continuous spiral-bed reactor, J. Mol. Catal. B: Enzym., 66 (2010) 302–310.
[27] M. Munichandran, B. Gangadhar, G. Naidu, Bioremoval of nickel and lead using bitter gourd (*Momordica charantia*) seeds, Int. J. Adv. Res. Sci. Eng. Technol., 3 (2016) 2475–2484.
[28] L.B.L. Lim, N. Priyantha, K.J. Mek, N.A.H.M. Zaidi, Potential use of *Momordica charantia* (bitter gourd) waste as a low-cost adsorbent to remove toxic crystal violet dye, Desal. Wat. Treat., 82 (2017) 121–130.
[29] M.K. Dahri, M.R.R. Kooh, L.B.L. Lim, Application of *Casuarina equisetifolia* needle for the removal of methylene blue and malachite green dyes from aqueous solution, Alexandria Eng. J., 54 (2015) 1253–1263.
[30] H.I. Chieng, N. Priyantha, L.B.L. Lim, Effective adsorption of toxic brilliant green from aqueous solution using peat of Brunei Darussalam: isotherms, thermodynamics, kinetics and regeneration studies, RSC Adv., 5 (2015) 34603–34615.
[31] N. Ara, M. Rahman, A. Alam, Effect of salts on the removal of remazol yellow by using activated charcoal prepared from sawdust, Bangladesh J. Sci. Ind. Res., 50 (2015) 285–292.
[32] K. Bharathi, S. Ramesh, Removal of dyes using agricultural waste as low-cost adsorbents: a review, Appl. Water Sci., 3 (2013) 773–790.
[33] I. Langmuir, The adsorption of gases on plane surfaces of glass, mica and platinum, J. Am. Chem. Soc., 40 (1918) 1361–1403.
[34] H. Freundlich, Over the adsorption in the solution, J. Phys. Chem., 57 (1906) 385–470.
[35] M. Temkin, V. Pyzhev, Kinetics of ammonia synthesis on promoted iron catalyst, Acta Phys. Chim. USSR, 12 (1940) 327–356.
[36] R. Sips, On the structure of a catalyst surface, J. Chem. Phys., 16 (1948) 490–495.
[37] O. Redlich, D.L. Peterson, A useful adsorption isotherm, J. Phys. Chem., 63 (1959) 1024–1024.
[38] N. Gupta, A.K. Kushwaha, M.C. Chattopadhyaya, Application of potato (*Solanum tuberosum*) plant wastes for the removal of methylene blue and malachite green dye from aqueous solution, Arabian J. Chem., 9 (2016) 707–716.
[39] A.S. Sartape, A.M. Mandhare, V.V. Jadhav, P.D. Raut, M.A. Anuse, S.S. Kolekar, Removal of malachite green dye from aqueous solution with adsorption technique using *Limonia acidissima* (wood apple) shell as low cost adsorbent, Arabian J. Chem., 10 (2017) 3229–3238.
[40] A.S. Franca, L.S. Oliveira, S.A. Saldanha, P.I.A. Santos, S.S. Salum, Malachite green adsorption by mango (*Mangifera indica* L.) seed husks: kinetic, equilibrium and thermodynamic studies, Desal. Wat. Treat., 19 (2010) 241–248.
[41] K.V. Kumar, Optimum sorption isotherm by linear and non-linear methods for malachite green onto lemon peel, Dyes Pigm., 74 (2007) 595–597.
[42] B.H. Hameed, M.I. El-Khaiary, Malachite green adsorption by rattan sawdust: isotherm, kinetic and mechanism modeling, J. Hazard. Mater., 159 (2008) 574–579.
[43] M.R.R. Kooh, L.B. Lim, L.H. Lim, J. Bandara, Batch adsorption studies on the removal of malachite green from water by chemically modified *Azolla pinnata*, Desal. Wat. Treat., 57 (2016) 14632–14646.
[44] B.H. Hameed, M.I. El-Khaiary, Kinetics and equilibrium studies of malachite green adsorption on rice straw-derived char, J. Hazard. Mater., 153 (2008) 701–708.

[45] R. Gong, Y. Jin, F. Chen, J. Chen, Z. Liu, Enhanced malachite green removal from aqueous solution by citric acid modified rice straw, J. Hazard. Mater., 137 (2006) 865–870.
[46] H.I. Chieng, T. Zehra, L.B.L. Lim, N. Priyantha, D.T.B. Tennakoon, Sorption characteristics of peat of Brunei Darussalam IV: equilibrium, thermodynamics and kinetics of adsorption of methylene blue and malachite green dyes from aqueous solution, Environ. Earth Sci., 72 (2014) 2263–2277.
[47] S. Agarwal, I. Tyagi, V.K. Gupta, S. Mashhadi, M. Ghasemi, Kinetics and thermodynamics of Malachite Green dye removal from aqueous phase using iron nanoparticles loaded on ash, J. Mol. Liq., 223 (2016) 1340–1347.
[48] K.V. Kumar, Comparative analysis of linear and non-linear method of estimating the sorption isotherm parameters for malachite green onto activated carbon, J. Hazard. Mater., 136 (2006) 197–202.
[49] H.I. Chieng, L.B.L. Lim, N. Priyantha, Enhancing adsorption capacity of toxic malachite green dye through chemically modified breadnut peel: equilibrium, thermodynamics, kinetics and regeneration studies, Environ. Technol., 36 (2015) 86–97.
[50] L.B.L. Lim, N. Priyantha, N.H. Mohd Mansor, Utilizing *Artocarpus altilis* (breadfruit) skin for the removal of malachite green: isotherm, kinetics, regeneration, and column studies, Desal. Wat. Treat., 57 (2016) 16601–16610.
[51] M.R.R. Kooh, M.K. Dahri, L.B.L. Lim, Jackfruit seed as low-cost adsorbent for removal of malachite green: artificial neural network and random forest approaches, Environ. Earth Sci., 77 (2018) 434.
[52] Y. Huang, M. Long, P. Liu, D. Chen, H. Chen, L. Gui, T. Liu, S. Yu, Effects of partition coefficients, diffusion coefficients, and solidification paths on microsegregation in Fe-based multinary alloy, Metall. Mater. Trans. B, 48 (2017) 2504–2515.
[53] S. Lagergren, About the theory of so-called adsorption of soluble substances, K. Sven. Vetenskapsakad. Handl., 24 (1898) 1–39.
[54] Y.S. Ho, G. McKay, Sorption of dye from aqueous solution by peat, Chem. Eng. J., 70 (1998) 115–124.
[55] W. Plazinski, W. Rudzinski, A. Plazinska, Theoretical models of sorption kinetics including a surface reaction mechanism: a review, Adv. Colloid Interface Sci., 152 (2009) 2–13.
[56] L.B.L. Lim, N. Priyantha, H.H. Cheng, N.A.H.M. Zaidi, Adsorption characteristics of *Artocarpus odoratissimus* leaf toward removal of toxic Crystal violet dye: isotherm, thermodynamics and regeneration studies, J. Environ. Biotechnol. Res., 4 (2016) 32–40.